AtomDB 2.0: Updated Atomic Data for X-ray Astrophysics

A. R. Foster, L. Ji, R. K. Smith and N. S. Brickhouse

Smithsonian Astrophysical Observatory, Cambridge, MA 02144, USA

Received ______________________; accepted ______________________

ABSTRACT

We describe the latest release of AtomDB (version 2.0), a database of atomic data and a plasma modeling code with a focus on X-ray astronomy. This release includes several major updates to the fundamental atomic structure and transition data held within AtomDB, incorporating new ionization balance data, state-selective recombination data, and updated collisional excitation data for many ions, including the iron L-shell ions from Fe^{+16} to Fe^{+23}. We also describe some of the effects that these changes have on calculated emission and diagnostic line ratios, such as changes in the temperature-dependent G-ratio for He-like ions of up to 33%. Finally, we compare observations of Capella using the new and the old datasets to show ???FIXME???.

1. Introduction

Analysis of astrophysical spectra recorded by instruments in X-ray and other wavelength bands is a powerful tool for understanding the composition and plasma conditions in a wide variety of astrophysical phenomena. Successful analysis of this data requires both a model of the plasma and a large selection of data detailing the various atomic processes occuring in the plasma.

The recognition of the importance of the dielectronic recombination (DR) process for plasmas, even at high temperatures, (Burgess 1964) led to huge strides in modeling collisionally ionized, optically thin astrophysical plasmas.: Cox & Tucker (1969) collated some of the earliest data. Since then there have been a steady stream of refinements to collisional models, usually incorporating improvements to either or both of the physical model (including more processes, for example), and the underlying data (using more accurate or more complete data sets). Different evolutions of such models have included those of Cox & Daltabuit (1971), Mewew (1972), Landini & Fossi (1972), Raymond & Smith (1977), and Brickhouse et al. (1995).

The quantity of relevant atomic data continues to grow as the computational power available for performing calculations improves. In modern analysis of X-ray astrophysical spectra there are three widely used atomic databases: XSPEC version 2.0.1 (Arnaud 1996), CHIANTI version 6.0.1 (Dere et al. 2009) and AtomDB version 1.3 (Smith & Brickhouse 2001). Each database has a slightly different focus: CHIANTI's main focuse is on the EUV wavelengths for analyzing solar spectra, while XSPEC and AtomDB focus on the X-ray ranges. These databases continue to undergo periodic review, and are updated as newer data become available; this paper introduces the release of version 2.0 of AtomDB, describing the new data and improvements, how they have been implemented and what is planned for future releases.

2. New Data

Changes have been made to large areas of the AtomDB database. Several ions which were not previously included are now in the database. Data for many other ions have been improved by including more recent calculation data, by increasing the number of energy levels and transitions included for the ion, or a combination of the both. In addition, major changes have been made to the ionization and, particularly, recombination data, with some significant changes to the resulting ionization balance and therefore to line emissivities. Here we outline each change in detail; in section 3 we will summarize the effect of these changes on the spectra observed by users. We note that in this release there are no changes to the format of the data files which the database uses and produces, which were described in Smith et al. (2001).

2.1. Ionization and Recombination Rates

While calculation of the ionization balance is just one part of calculating an emission spectrum for a plasma, it has a very strong effect on the result. As experimental and theoretical methods improve, there are periodical efforts to collect the rates for ionization and recombination, both radiative (RR) and dielectronic (DR), for easy use by astrophysicists. Previous examples include the widely used data sets of Arnaud & Raymond (1992) and Mazzotta et al. (1998): the latter was included in AtomDB 1.3. Bryans et al. (2006, 2009) have produced a new compilation of ionization balance data for elements from hydrogen ($Z_0 = 1$) to zinc (Z_0=30), and this has been included in AtomDB v2.0. This dataset provides new rates for DR and RR for all astrophysically relevant ions from fully stripped up to Na-like systems (where Na-like refers to the recombining ion): for the remaining ions, the data of Mazzotta et al. (1998) is retained. In addition, the Bryans et al. (2009) data includes collisional ionization from Dere (2007) for all ions.

In their papers Bryans et al. (2006, 2009) compare the ionization and recombination data with the earlier data sets and with experimental measurements. While the electron impact ionization (EII) and RR rates have not changed dramatically, for many L-shell ions there have been significant changes in the DR rates. The DR and RR calculations now generally agree to within 35% of available measurements. For EII there is disagreement for some heavier, lightly ionized ions (Mg-like and above) between the results of Dere (2007) and Mattioli (2007), the former has been included here as incorporated in the Bryans data set: hopefully further study will provide further enlightenment as to the correct values.

The Badnell (2006) data sets which Bryans used for the DR and RR rates are part of a compilation which is undergoes periodic update and review. Since their publication in 2006, the rates for DR into nitrogen-like ions have been revised; we have included this revised data here. For all other ions the DR & RR rates are the same as those of Bryans et al. (2009).

2.2. State-Selective DR & RR Rates

The DR and RR data in the Bryans et al. (2006) collection give total rates for recombination from the ground state of one ion to the next. The Badnell (2006) calculations on which these are based are resolved into state-selective recombination rates, so that the recombination rate into each excited state of the ion is specified. This allows inclusion of these direct rates when calculating the excited-state populations of the recombined ion, and as a result will affect emission lines, particularly in regions of strong DR (see examples in Section 3.5). For this reason we have included state-selective data for recombination to all H-like, He-like and Li-like ions, and all iron ions from Fe^{+16} to Fe^{+22}.

The DR & RR source data are split into level-resolved rates for capture into lower n (typically $n \leq 8$), with capture rates into higher n provided as totals into each n-shell. Since the levels identified in the DR & RR calculations and those in AtomDB are rarely identical, some level matching and cascade calculations have been required.

This has been achieved with a several step process. Using the AUTOSTRUCTURE (Badnell 1986) code, transition probabilities have been calculated for all the energy levels which appear in either the AtomDB datasets or the DR/RR calculations. In addition, transition probabilities between n shells have been estimated using the hydrogenic approximation of Burgess & Summers (1976). Using this data, the capture into the high-n levels has been cascaded down, assuming zero electron density and thus no collisional re-ionization/re-distribution effects, to the lower n levels for which resolved data exists. The cascade contribution is then distributed according to the statistical weight of each level within the n shell.

The Einstein A-values from Autostructure are then used to further cascade the data as required from these levels until levels which are in the AtomDB database for collisional excitation are encoutered. Thus a total effective recombination rate to each level in the AtomDB database is constructed from a direct rate and cascade from higher n levels.

This treatment of the cascade process does cause certain omissions which we hope to address in future: firstly, the photons emitted during the cascade are not tracked and therefore are not included in any spectral models or radiated power estimates. In addition, the treatment of DR satellite lines in not consistent with this information: those lines are tabulated as a function of temperature obtained from separate calculations: these would be better handled in a self consistent manner during the original calculation of the DR rates. Future work will aim to address these problems.

2.3. H-like Ions

The data for hydrogenic ions have been upgraded in two major ways: (1) extended to include higher n-shells (from $n_{upper} = 5$ to $n_{upper} = 10$), and, (2) where available, data of a higher quality have been used for ions of astrophysical interest.

Due to the simplicity of the hydrogenic system, it is often used as a training case when learning R-Matrix techniques or other sophisticated collional techniques. However, due to the assumed simplicity of the system, it is rare for the data to be actually recorded. The ions for which modern H-like R-Matrix collision strengths could be obtained are shown in Table 1. The atomic structure and A-values for the higher-n data were obtained using Autostructure. The electron impact excitation data for these higher n was calculated using the Flexible Atomic Code (FAC, Gu (2003)). R-Matrix calculations exist for collisional excitation for transitions with $n_{upper} \leq 5$ for several ions. These calculations have been performed in LS coupling, not LSJ for all such ions except Fe^{+25} (see Table 1). LS coupling is sufficient for most of the lighter ions as the relativistic splitting between J-resolved levels is not generally observable: an energy resolution $E/\Delta E > 2000$@1 keV is required to observe the $2p^2P_{[1/2,3/2]} \rightarrow 1s^1S$ splitting of Neon; for lighter elements it is higher.

The possible advent of higher resolution detectors in the future means that AtomDB is targeted at LSJ resolved data throughout: all other data in the database is already LSJ resolved. We therefore have used a combination of AUTOSTRUCTUREfor exnergy levels and A-values, with collisional excitation rates from FAC, to create the data for AtomDB. The exception here is for excitation from ns levels, for which the R-matrix collision strength has been used, split by the statistical weight of the final state.

For completeness, for all ions not mentioned in Table 1, data were produced using AUTOSTRUCTURE for energy levels and transition probabilities, and using FAC for the collision strengths for all energy levels with $n_{upper} \leq 10$.

2.4. He-like ions

For the He-like ions, data have been incorporated from new Intermediate Coupling Frame Transformation (ICFT) R-Matrix (Griffin et al. 1998) calculations provided by Whiteford (2005) for all elements from C^{5+} to Kr^{35+}. In this work, structure data is again generated by AUTOSTRUCTURE, with the ICFT method being used for the collision strengths. As with the H-like ions we have extended the range of these calculations using FAC to obtain collision strengths for collisions with $5 < n_{upper} \leq 10$.

2.5. Iron L-shell Data

For the iron L-shell ions (Fe^{+16} to Fe^{+23}) significant advances have been made in collisional excitation calculations since the release of AtomDB 1.3. The collision strength data for these ions have been upgraded to R-matrix calculations. Details of which particular calculation were used for each ion are given in Table 2. These new calculations include, in general, fewer configurations than the existing Distorted Wave data (Liedahl 1997) in AtomDB. As a result the newer data have been merged with the existing data, updating or adding as appropriate. Much of the older data remains for transitions involving some levels not included in the newer data.

2.6. Non-X-ray focused Data

For many other ions, especially those that are not notably strong emitters in the X-ray region, AtomDB version 1.3 used data from CHIANTI version 2.0 (Landi et al. 1999). We have updated the wavelengths, transition probabilities and collision strengths of all data for all ions excluding the H-like & He-like sequences, and the Ni and Fe L-shell ions to now incorporate the CHIANTI version 6.0.1 data (Dere et al. 2009).

2.7. Minor Changes

In addition to these major updates to the database, several minor corrections have been made which have little or no effect on the resulting spectra from AtomDB but which do affect the database. This includes the correct use of L and S quantum numbers for all levels where LS or LSJ coupling is used; consistent formatting of configuration strings, minor corrections to the H-like two-photon transition rate from the $2s^1 \rightarrow 1s^1$ level, including adding the rate for hydrogen and reducing it for all other hydrogenic ions.

Ion	Reference	n_{max}	Coupling
H^0	Anderson et al. (2002)	5	LS
He^+	Ballance et al. (2003)	5	LS
Li^{+2}	Ballance et al. (2003)	5	LS
Be^{+3}	Ballance et al. (2003)	5	LS
B^{+4}	Ballance et al. (2003)	5	LS
C^{+5}	Ballance et al. (2003)	5	LS
O^{+7}	Ballance et al. (2003)	5	LS
Ne^{+9}	Ballance et al. (2003)	6	LS
Fe^{+25}	Ballance et al. (2003)	5	IC

Table 1: The sources of data and maximum n shells for R-Matrix collisional calculations of H-like ions.

Ion	Reference	n_{max}
Fe^{+16}	Loch et al. (2006)	4
Fe^{+17}	Witthoeft et al. (2007a)	4
Fe^{+18}	Butler & Badnell (2008)	4
Fe^{+19}	Witthoeft et al. (2007b)	4
Fe^{+20}	Badnell & Griffin (2001)	4
Fe^{+21}	Badnell et al. (2001)	4
Fe^{+22}	Chidichimo et al. (2005)†	4
Fe^{+23}	Whiteford (2002)	3

Table 2: The data sources used for iron L-shell ions, and the maximum n shell included for each. † - as amended by Chidichimo & Mason (2005).

3. Results

3.1. New Ionization and Recombination rates

The effect of the new ionization data is most significant for heavier elements. Detailed information can be found in the papers of Bryans et al. (2006, 2009). In Figure 1 we show the change in the ionization balance for iron, including our use of different recombination rates for Fe XIX as specified in Section 2.1. Significant changes can be seen around Fe XVII, in some cases leading to changes in fractional abundance of upwards if 30%: this has in turn significant effects on emission lines present at these temperatures.

3.2. Total Radiated Power

Figure 2 shows the total power radiated from all elements given a solar elemental abundance (Anders & Grevesse 1989) and an electron density of $1\mathrm{cm}^{-3}$. The top figure shows a comparison between the total emission from the old and new versions of the database: as can be seen, there are significant ($> 10\%$) increases in radiation in four different temperature ranges. The increase at 2×10^4K is due to the inclusion of two-photon emission from hydrogen for the first time (this falls outside the traditional X-ray band and so was previously omitted). The remaining three increases are due to changes in the ionization balance for oxygen, neon and iron respectively: the new data have a higher fraction of less ionized ions present, which radiate more strongly in these hotter regions. The lower part of Figure 2 shows the radiation from each element, with the dominant element noted in each region.

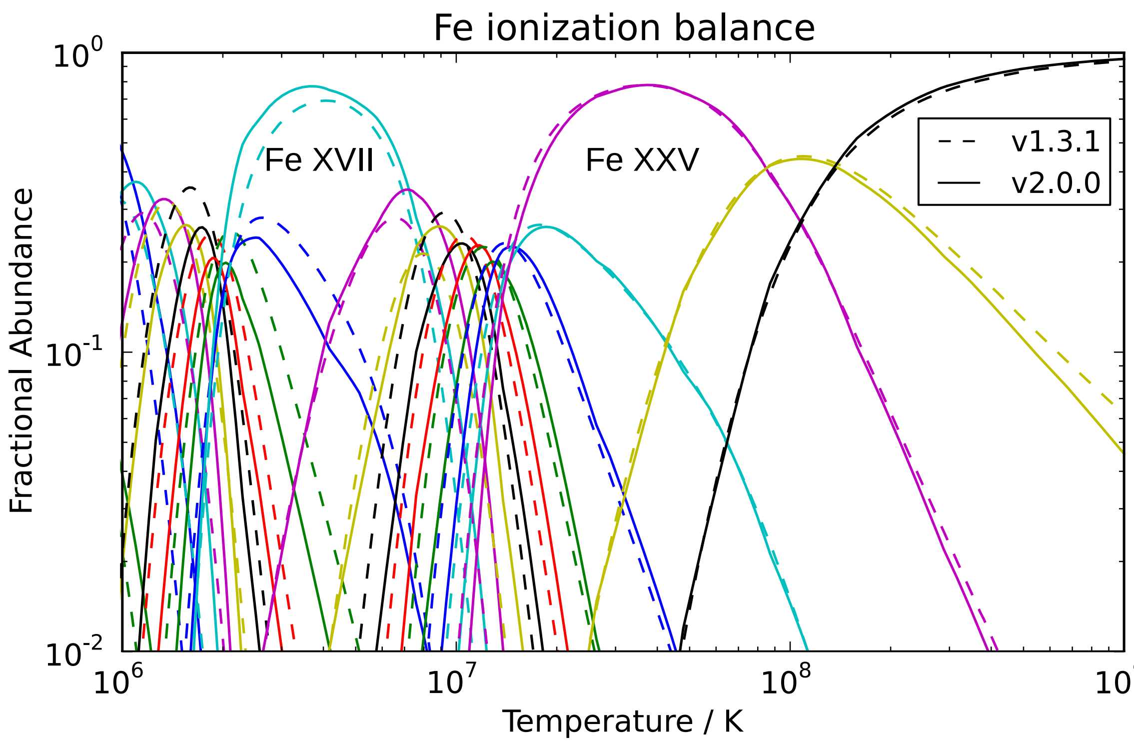

Fig. 1.— The ionization balance for iron about 10^6K. The dashed line is the Mazzotta et al. (1998) data used in AtomDB version 1.3, the solid line is the newer data mostly based on Bryans et al. (2006, 2009) included in version 2.0.

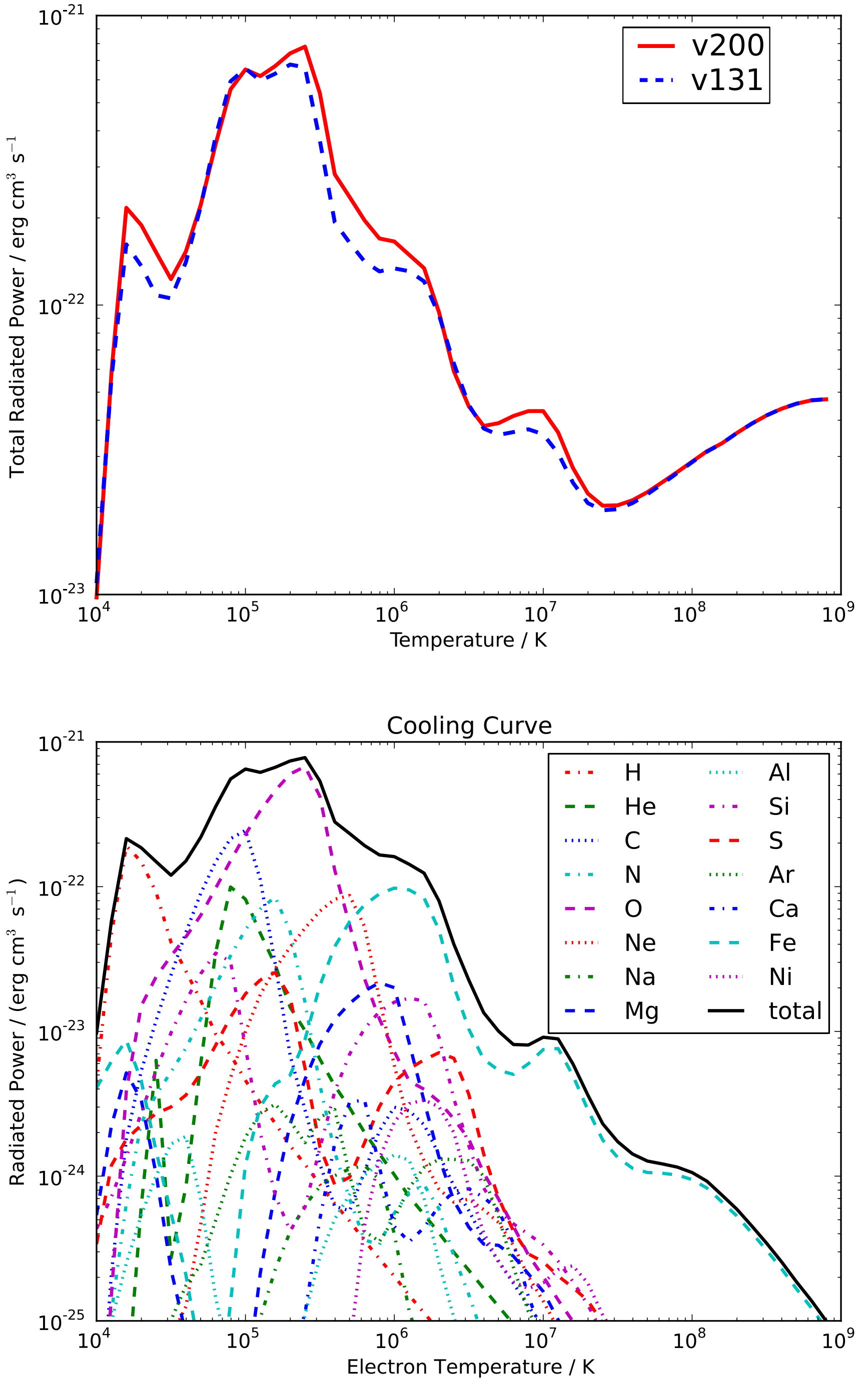

Fig. 2.— *Top:* the total radiated power in the 0.001 to 50keV band from all ions, assuming solar abundances, comparing the old (v1.3, dashed) and new (v2.0, solid) versions of AtomDB. *Bottom* The radiated power for AtomDB v2.0, broken down by element.

3.3. Higher n-shell Effects

The inclusion of higher n-shells for H- and He-like systems means that lines from such systems are now apparent. The effects on observations could be twofold: as well as new lines being observed, cascade effects to lower n could also alter line intensities. Figure 3 shows the emissivities of lines of Ne X, with the higher n-shell lines apparent, and demonstrates the possibility of observing these lines in sensitive observations with existing instrumentation.

3.4. Diagnostic Line Ratios

The replacement of the collisional excitation data for He-like ions leads to a significant change in the temperature-sensitive G-ratio (Gabriel & Jordan 1969). This is the ratio of emission from the forbidden and intercombination lines to the resonance lines. The changes can be seen in Figure 4; for most ions the G ratio substantially increases, in some cases by over a third. Problems with these line ratios have been known about for some time (Testa et al. 2004). In the case of Ne IX, calculations were carried out by Smith et al. (2009) to rectify this problem: the data here agrees well in this case, which gives confidence that the new data is correct. These new ratios will have a significant effect on estimating plasma temperatures for those cases where such line ratios were relied upon.

3.5. Spectra...

FIXME In here go comparisons of new and old spectra, to show how much things have (or haven't) changed. Plan to show new and old at CCD resolution for whole spectrum, and the He-like triplets new and old overlaid. Li is working on this... (thanks Li!).

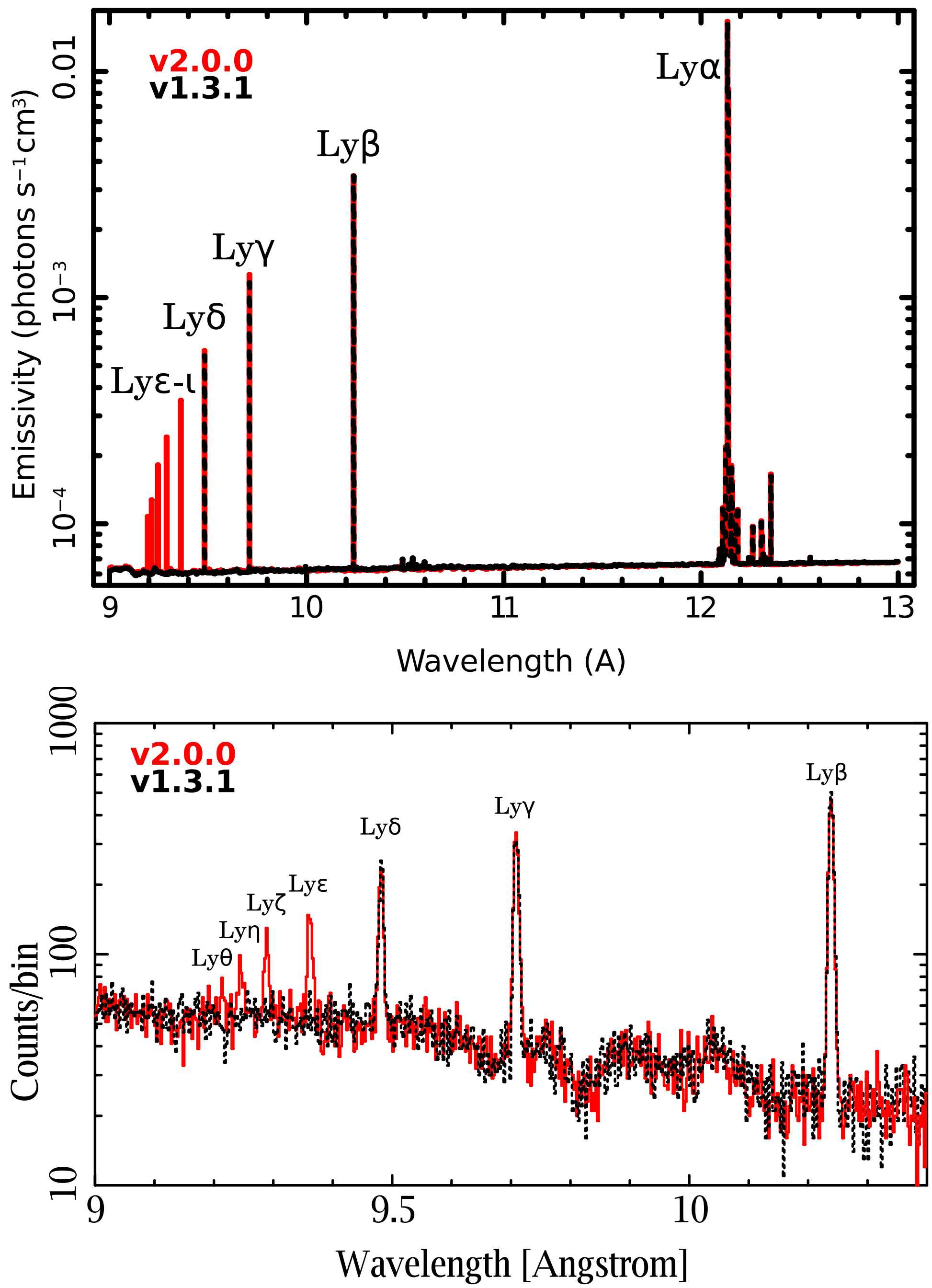

Fig. 3.— *Top:* the line emissivities for Ne X at 10^7K, showing the old data (dashed line) and the new (solid). The lines from the high-n cascade can be seen clearly. *Bottom:* A simulated spectrum of Ne X from a 100ks Chandra HETG observation, also at 10^7K.

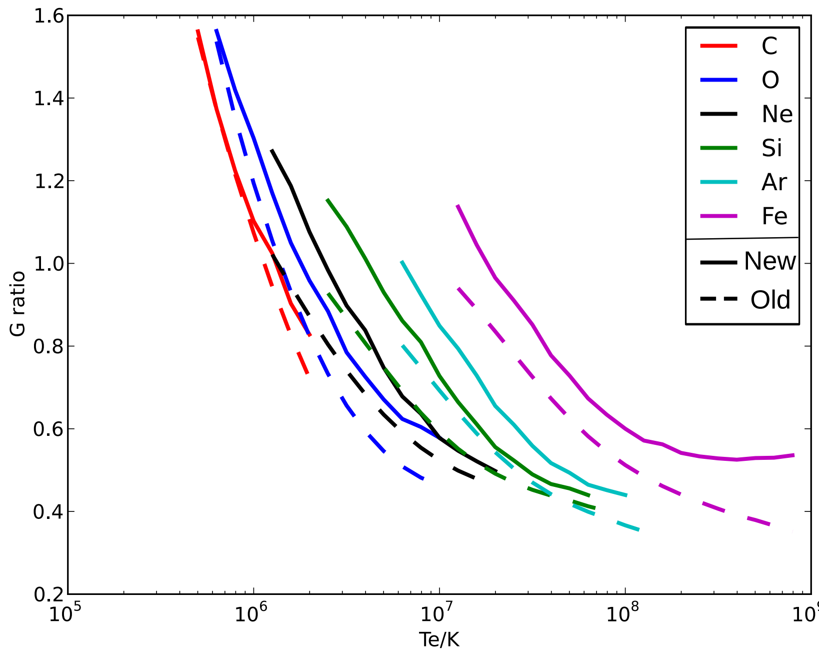

Fig. 4.— The temperature sensitive G=(F+I)/R ratio for selected He-like ions, for both the old (v1.3, dashed) and new (v2.0, solid) AtomDB releases.

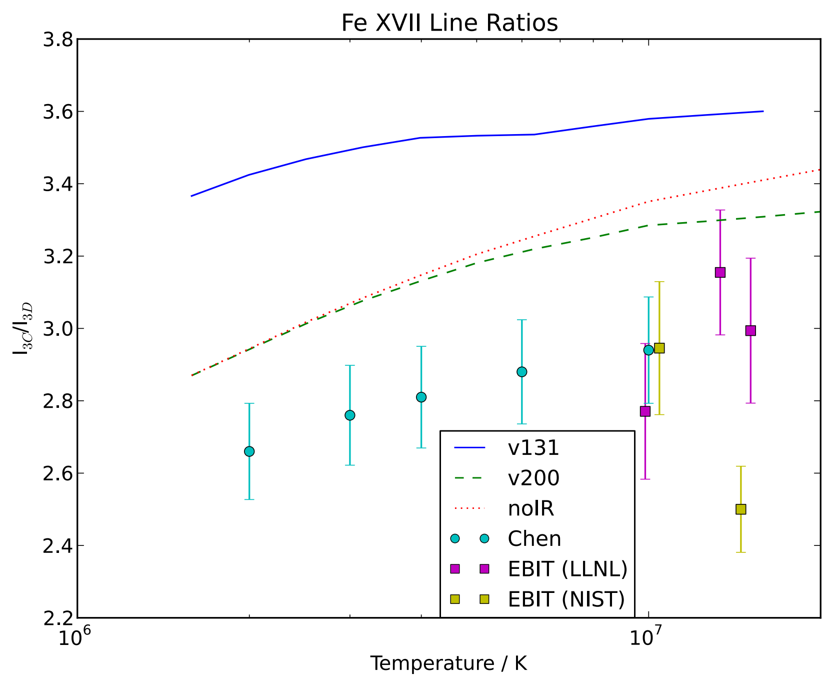

Fig. 5.— The Fe XVII 3C/3D line ratio from various sources: solid line: AtomDB v1.3; dashed line: AtomDB v2.0; dotted line: AtomDB v2.0, but excluding state-selective recombination; circles: Calculations of Chen (2008); squares: EBIT measurements.

4. Future Plans

There are several improvements already planned for the next release of AtomDB. These are largely centered around dielectronic recombination. We will aim to include state-selective DR rates for the remaining ions in the database. We will also re-write several stages of the plasma code to allow us to store the power lost during the radiative cascade of electrons from very high n shells during DR. We will also recalculate the DR satellite line emission so that we will have a more consistent picture of the emission and recombination rates.

5. Summary

We have presented the latest version of AtomDB, the first update since 2001. The data is now available online at www.atomdb.org, ready for use. We have outlined the effects of the changes on several plasma emission cases, and concluded that... FIXME

The authors gratefully acknowledge funding from NASA ADP grant #NNX09AC71G.

REFERENCES

Anders, E., Grevesse, N., 1989, Geochimica et Cosmochimica Acta, 53, 197

Anderson, H., Ballance, C. P., Badnell, N. R., Summers, H. P. 2002, J. Phys. B, 35, 1613

Arnaud, K.A., 1996, Astronomical Data Analysis Software and Systems V, eds. Jacoby G. and Barnes J., 17, ASP Conf. Series volume 101.

Arnaud, M., Raymond, J. C. 1992, ApJ, 398, 394

Badnell, N. R., 1986, J. Phys. B, 19, 3827

Badnell, N. R., Griffin, D. C. 2001 J. Phys. B, 34 681

Badnell, N. R., Griffin, D. C., Mitnik, D. M. 2001 J. Phys. B, 34, 5071

Badnell, N. R. 2006 Atomic and Molecular Diagnostic Processes in Plasmas (Dept. Physics, Univ. Strathclyde), http://amdpp.phys.strath.ac.uk/tamoc/DATA/

Ballance, C. P., Badnell, N. R., Smyth, E. S. 2003, J. Phys. B, 36, 3707

Brickhouse, N. S., Raymond, J. C., Smith, B. W. 1995, ApJS, 97, 551

Bryans, P., Badnell, N. R., Gorczyca, T. W., Laming, J. M., Witthumsiri, W., Savin, D. W. 2006, ApJS, 167, 343

Bryans, P., Landi, E., Savin, D. W. 2009, ApJ, 691, 1540

Burgess A. 1964, ApJ, 139, 776

Burgess, A. Summers, H. P. 1976, MNRAS, 174, 345

Butler, K. Badnell, N. R. 2008, A&A, 489, 1369

Chen, G. X., 2008, MNRAS, 386, L62

Chidichimo,M. C., Del Zanna, G., Mason, H.E., Badnell, N. R., Tully, J.A., Berrington, K.A., 2005, A&A, 430, 331

Chidichimo,M. C., Mason, H.E., 2005, A&A, 432, 1137

Cox, D. P., Tucker, W. H. 1969, ApJ, 157, 1157

Cox, D. P., Daltabuit, E. 1971, ApJ, 167, 113

Dere, K. P. 2007, A&A, 466, 771

Dere, K. P. et al. 2009, A&A, 498, 915

Gabriel, A. H., Jordan, C., 1969, MNRAS, 145, 241

Griffin, D. C., Badnell, N. R. Pindzola, M. S. 1998, J. Phys. B, 31, 3713

Gu, M. 2003 ApJ, 582, 1241

Landi, E., Landini, M., Dere, K.P., Young, P.R. Mason, H. E. 1999 A&AS, 135, 339

Landini, M., Monsignori Fossi, B. C. 1972, A&AS, 7, 291

Liedahl, D., private communication

Loch, S. D., Pindzola, M. S., Ballance, C. P., Griffin, D. C. 2006 J. Phys. B, 39, 85

Mattioli, M., et al. 2007, J. Phys. B, 40, 3569

Mazzotta, P., Mazzitelli, G., Colafrancesco, S., Vittorio, N. 1998, A&AS, 133, 403

Mewe, R. 1972, Sol. Phys., 22, 459

Raymond, J. C., Smith, B. 1977, ApJS, 35, 419

Smith, R. K., Brickhouse, N. S., Liedahl, D. A., Raymond, J. C., 2001, in Spectroscopic Challenges of Photoionized Plasmas, ASP Conference Series, eds. Ferland, G. Savin, D., v247 p 161

Smith, R. K., Brickhouse, N. S., Liedahl, D. A., Raymond, J. C., 2001, ApJ, 556, L91

Smith, R. K., Chen, G.-X., Kirby, K., Brickhouse, N. S., 2009 ApJ, 700, 679.

Testa, P., Drake, J. J., Peres, G., 2004 ApJ, 617, 508.

Whiteford, A. D., Badnell, N. R., Ballance, C. P., Loch, S. D., Mullane, M. G., Summers, H. P., 2002 J. Phys. B, 35, 3729

Whiteford, A. D., private communication

Witthoeft, M. C., Whiteford, A. D., Badnell, N. R. 2007 J. Phys. B, 40, 2969

Witthoeft, M. C., Del Zanna, G., Badnell, N. R. 2007 A&A, 466, 763

This manuscript was prepared with the AAS LaTeX macros v5.2.